



Letter

Magnetoimpedance Response and Field Sensitivity in Stress-Annealed Co-Based Microwires for Sensor Applications

David González-Alonso ¹, Lorena González-Legarreta ^{2,3,*}, Paula Corte-León ^{3,4},
Valentina Zhukova ^{3,4} , Mihail Ipatov ^{3,4}, Juan María Blanco ⁴ and Arcady Zhukov ^{3,4,5,*} 

¹ Departamento CITIMAC, Facultad de Ciencias, Universidad de Cantabria, E-39005 Santander, Spain; david.gonzalezalonso@unican.es

² Departamento QUIPRE, Inorganic Chemistry-University of Cantabria, Nanomedice-IDIVAL, Avda. de Los Castros 46, 39005 Santander, Spain

³ Departamento de Física de Materiales, Facultad de Químicas, Universidad del País Vasco/Euskal Herriko Unibersitatea, UPV/EHU, Paseo Manuel de Lardizabal, 3, 20018 San Sebastián, Spain; paula.corte@ehu.eus (P.C.-L.); valentina.zhukova@ehu.es (V.Z.); mihail.ipatov@ehu.es (M.I.)

⁴ Departamento de Física Aplicada, EIG, Universidad del País Vasco/Euskal Herriko Unibersitatea, UPV/EHU, 20018 San Sebastian, Spain; juanmaria.blanco@ehu.es

⁵ IKERBASQUE, Basque Foundation for Science, 48011 Bilbao, Spain

* Correspondence: gonzalezll@unican.es (L.G.-L.); arkadi.joukov@ehu.es (A.Z.)

Received: 17 May 2020; Accepted: 3 June 2020; Published: 5 June 2020



Abstract: Amorphous soft magnetic microwires have attracted much attention in the area of sensor applications due to their excellent properties. In this work, we study the influence of annealing treatments (stress and conventional) in the giant magnetoimpedance (GMI) response and the field sensitivity of the soft magnetic $\text{Co}_{69.2}\text{Fe}_{3.6}\text{Ni}_{1}\text{B}_{12.5}\text{Si}_{11}\text{Mo}_{1.5}\text{C}_{1.2}$ glass-coated microwires. Here we report a remarkable and simultaneous enhancement of GMI effect and field sensitivity. The highest sensitivity of 104%/Oe and the GMI response of 234% were achieved for 300 °C stress-annealed samples at 472 and 236 MPa, respectively. Additionally, we found that stress-annealed microwires exhibit a frequency dependence on maximal GMI response and field sensitivity. These findings are obtained by fine-tuning their magnetoelastic anisotropies through stress-annealing treatments of as-prepared microwires at the proper temperature and axial applied stress upon annealing. We hope that the results presented here widen the scope of investigations for the future design of soft magnetic materials for sensor purposes.

Keywords: magnetoimpedance effect; skin effect; soft magnetic materials; field sensitivity; amorphous microwires

1. Introduction

Over the last decades, magnetic sensors have captivated scientific attention for their technological findings in a broad scope of fields. These applications range from space research, military applications, security systems, high-density magnetic recording and biomedicine [1–6]. In this line, the miniaturization of sensors and technological devices opens new routes in the property-to-function conversion. Metal-based amorphous alloys [7,8] constitute the main family within magnetic sensors. After Panina et al. [7,8], Co-based rapidly quenched materials have become widely recognized magnetic materials for sensors due to their high-performance properties [9,10]. It should be highlighted that their excellent magnetic softness, exhibiting nearly zero magnetostriction constant value and a

remarkably giant magnetoimpedance (GMI) response along with high field sensitivity, among other properties [7,11,12].

In this sense, giant magnetoimpedance (GMI) effect results is the most remarkable feature for sensor applications. This phenomenon consists in a significant change of the AC impedance in presence of a static dc-field [13]. GMI ratios up to 600%, at frequencies around 10 MHz [14] and sensitivities up to $10\%/Am^{-1}$ are the maximum values reported to date for amorphous wires [15]. These properties make Co-based materials quite suitable candidates for GMI technology, such as magnetic field sensors integrated in complementary metal-oxide-semiconductor (CMOS) circuits [16], high sensitive magnetometers [17] or biomagnetic field detection [18,19].

Co-based glass-coated microwires are attracting scientific interest for their potential in the development of small-scale sensors based on their tunable magnetic properties. The Co-based microwires investigated in this work are fabricated by the Taylor-Ulitovsky technique [20,21]. The Taylor-Ulitovsky technique involving rapid solidification of metallic alloys inside the glass coating allows the preparation of long (up to 10 km) continuous composite metallic microwires coated by a flexible and insulating glass cover (typical thickness of 0.5–20 μm). At suitable fabrication conditions, a completely amorphous structure with no trace of crystalline phases can be obtained [20,21]. Magnetocrystalline anisotropy contribution is consequently negligible, while their magnetic properties are principally governed by the magnetoelastic interactions. Furthermore, the magnetoelastic interactions play a key role in the GMI response [15,21,22]. In fact, these interactions are determined by both the magnetostriction coefficient and internal stresses [23]. Apart from these contributions, classical electrodynamics gives the fundamental support to explain satisfactorily the GMI effect by considering the skin effect of a magnetic conductor [24]. Based on this assumption, the most relevant pre-requisite to achieve a giant MI response is to design amorphous microwires with significant circumferential magnetic permeability, which can be reached by fine-tuning their magnetic properties [25–27].

With respect to the magnetoelastic anisotropy of glass-coated microwires, the magnetostriction coefficient, λ_s , is dictated by the chemical composition (at fixed internal stresses values which in turn are affected by the fabrication conditions) [28]. Thus, the replacement of Fe by Co atoms permits the adjustment of λ_s -values from positive (typically $\lambda_s \sim 40 \times 10^{-6}$ for Fe-based microwires) to negative (about $\lambda_s \sim -5 \times 10^{-6}$ for Co-based microwires) values [28,29]. Accordingly, the vanishing λ_s -values can be achieved in Co-Fe or Co-Mn amorphous alloys when the content of Co/Fe or Co/Mn is about 70/5 [28,29]. Moreover, for alloys with vanishing λ_s -values the stresses influence can be relevant [28]. On the other hand, the internal stresses (value and distribution), which arise from the fabrication of glass-coated microwires, are the other factor affecting the magnetoelastic anisotropy [15,21,23]. The internal stresses, σ_i , value can be caused by: i) the thermal expansion coefficient mismatch between metallic-core and the glass-coating; ii) the quenching stresses originated during the rapid solidification process; and iii) the drawing stresses [30,31]. According to most theoretical estimations, the internal stresses arising from the thermal expansion coefficient mismatch are expected to present the largest contribution [30,31].

In this regard, at a fixed composition and geometry (metallic nucleus diameter and glass-coating thickness) the magnetic anisotropy can be fine-tuned either by the internal stresses relaxation (usually by conventional annealing) or by inducing magnetic anisotropy [27,32]. However, it has been recently noticed that conventional annealing produces a considerable magnetic hardening in different Co-rich microwires with vanishing λ_s -values [32,33]. Such magnetic hardening is a detriment to the GMI performance [27,32,33]. Nevertheless, we have recently observed that stress-annealing can be successfully employed to induce a transverse anisotropy and hence improve the GMI effect of magnetic microwires [27,32,33].

For those reasons, our aim is to identify the routes that allow the optimization of GMI performance at a fixed chemical composition and geometry (i.e., with fixed λ_s and σ_i values). We expect that in the future the observed dependencies can be extended to various Co-rich microwires.

Accordingly, in this work, we have investigated the magnetic properties of Co-based amorphous microwires with a well-established chemical composition under stress-annealing conditions aiming to simultaneously enhance their GMI response and magnetic field sensitivity within the range $10 \leq f \leq 1000$ MHz of intermediate frequencies.

2. Experimental Methods

The $\text{Co}_{69.2}\text{Fe}_{3.6}\text{Ni}_1\text{B}_{12.5}\text{Si}_{11}\text{Mo}_{1.5}\text{C}_{1.2}$ microwire consists in a metallic nucleus of $d = 22.8 \mu\text{m}$ diameter, surrounded by an outer glass-coating shell that results in $D = 23.2 \mu\text{m}$ total diameter. The amorphous microwire has been fabricated using the Taylor-Ulitovsky technique, which is described elsewhere [20,21]. As in similar Co-based microwires [28], the sample presents a slightly negative magnetostriction coefficient $\lambda_S \approx -1 \times 10^{-7}$ [27]. This allows us to predict the magnetic softness in our sample and suggests the existence of a circumferential anisotropy along the microwire. This latter feature is the underlying ingredient to obtain remarkable MI response [24,34].

For proper modification to the magnetic properties of our sample, slices of the as-prepared microwire were subsequently heat-treated in a standard furnace by two different methods. In one method the annealing is performed with no applied stress, whereas in the second it is conducted under axial tensile stress. The tensile stress, σ_m , was applied through a mechanical load attached to the end of the microwire and axially placed via the furnace nozzle, allowing stresses up to 472 MPa. The σ_m -values are evaluated considering the different Young's moduli of the metallic nucleus and the glass coating as recently described [33]. All these treatments were performed at selected temperatures, T_{ann} , ranged from 200 to 400 °C and for 1 h duration, t_{ann} . This annealing temperature range has been selected considering the onset of the crystallization process reported at ca. 490 °C for microwires of the same composition [35]. In fact, it has been described that the rising of the annealing temperature close to the crystallization point causes a deterioration of both mechanical and magnetic properties in Co-rich microwires [36,37]. Although two of the advantages of glass-coated microwires are their flexibility and insulating properties of the glass coating, an excess of temperature can damage the outer glass-coating.

Magnetic hysteresis loops (HLs) were measured using the fluxmetric method already described [33]. Microwire slices of 5 cm in length were placed inside a single layered pick-up coil, where a magnetic field was created by a 15 cm long solenoid. For better comparison of the treated microwires, HLs are represented as the normalized magnetization M/M_0 , where M is the measured magnetic moment at a given magnetic field, and M_0 is the maximal magnetic moment obtained at the highest magnetic field amplitude H_{max} .

Impedance measurements, Z , were carried out with a vector network analyzer (VNA) N5230A at room temperature. Microwires of 6 mm length were fixed to a micro-strip sample holder by tin soldering, and subsequently placed inside a long solenoid that creates a maximum homogeneous magnetic field, H , of 15 kA/m (ca. 189 Oe). Z -values are indirectly obtained in the intermediate frequency range 10–1000 MHz through the measurement of the reflection coefficient S_{11} , using the following expression [34,38]:

$$Z = Z_0 \frac{(1 + S_{11})}{(1 - S_{11})} \quad (1)$$

where $Z_0 = 50 \text{ Ohm}$ is the characteristic impedance of the coaxial line.

The MI response or GMI ratio, $\Delta Z/Z$, is determined from Z -values, which are obtained for different magnetic fields measurements, and it is defined as:

$$\Delta Z/Z = \frac{[Z(H) - Z(H_{max})]}{Z(H_{max})} \times 100 \quad (2)$$

where H_{max} is the highest dc-magnetic field applied.

A distinctive feature of MI response to discriminate among magnetic sensor materials is the field sensitivity, η , which is calculated through:

$$\eta = \frac{\partial\left(\frac{\Delta Z}{Z}\right)}{\partial H} \quad (3)$$

3. Results and Discussion

The MI response in amorphous ferromagnetic microwires can be enhanced by relaxing their inner stresses through a diversity of thermal treatments. In view of this, we present here the advantages of stress-annealing when optimising the magnetic properties of the $\text{Co}_{69.2}\text{Fe}_{3.6}\text{Ni}_1\text{B}_{12.5}\text{Si}_{11}\text{Mo}_{1.5}\text{C}_{1.2}$ as-prepared microwire, in contrast to conventional annealing. Figure 1a shows the HLs of the as-prepared, along with the annealed microwires performed at selected temperatures T_{ann} below its crystallization point ($\sim 550^\circ\text{C}$, [35]). In the inset of Figure 1a, it is observed a magnetic hardening after 1h annealing. Particularly, in Figure 2a we depict the effect of conventional annealing by increasing the H_c from ca. 0.06Oe (5 A/m) for the as-prepared sample, up to ca. 1.26 Oe (100 A/m) for the conventional annealed microwire at the highest T_{ann} of 400°C .

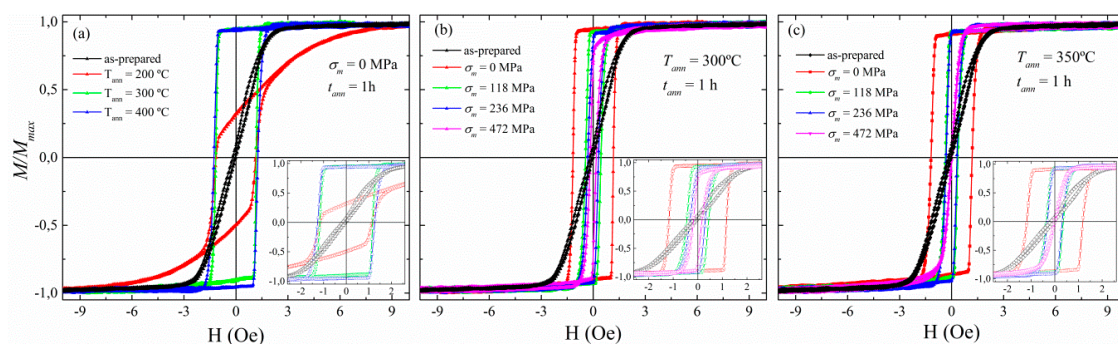


Figure 1. (a) Hysteresis loops (HLs) of the as-prepared and the annealed microwires performed at 200°C , 300°C , and 400°C . Subfigures (b) and (c) show HLs of as-prepared and stress-annealed performed at $T_{ann} = 300$ and 350°C , respectively. The thermal treatments on the parent-microwire $\text{Co}_{69.2}\text{Fe}_{3.6}\text{Ni}_1\text{B}_{12.5}\text{Si}_{11}\text{Mo}_{1.5}\text{C}_{1.2}$ were performed for 1h. In the insets, it is shown a magnification of the HLs to make clear the linear-to-rectangular evolution of the treated microwires.

The effect of conventional annealing on HLs of Co-rich microwires with low-negative magnetostriction λ_s has already been studied [23]. Conventional annealing is expected to produce magnetic hardening, along with an increment in the magnetization of the metallic nucleus as evinced in the linear-to-rectangular evolution of the HLs in Figure 1a as T_{ann} rises. The magnetic hardening is explained through internal stresses relaxation that brings about circumferential domain structure along the microwire. This hardening could also be the result of either a growth of inner axially magnetized domains [21,26,38], or a variation in the magnetostriction value [39,40], or even a sign change in the magnetostriction coefficient [23,40,41].

Hence, conventional annealing cannot be considered the best post-processing treatment to improve magnetic softness of Co-based microwires. In this regard, stress-annealing counteracts the magnetic hardening experienced by the microwire on conventional annealing. This effect is plainly visible in the insets of Figure 1b,c, where two characteristic stress-annealing temperatures are represented, $T_{ann} = 300$ and 350°C , respectively. There, the coercive field, H_c , is reduced while achieving a magnetic softening, which is more clearly shown in Figure 2b. In addition, microwire soft magnetic properties can be affected by the stress-annealed conditions, i.e., T_{ann} , t_{ann} and σ_m [27,33,40,41]. Figure 1c shows that the linear HLs typically observed for the as-prepared microwire are recovered at high enough T_{ann} and σ_m (in violet), but at the expense of M_r/M_0 -values (where M_r is the remanent magnetization). This decrease in the M_r/M_0 ratio results in a reduction of the GMI response as is observed below for the

stress-annealed microwire at $T_{ann} = 300$ °C and $\sigma_m = 472$ MPa. These changes of magnetic properties result from an increase in circumferential magnetic anisotropy, which is induced by stress-annealing and becomes more significant when increasing T_{ann} , t_{ann} and σ_m [33,38].

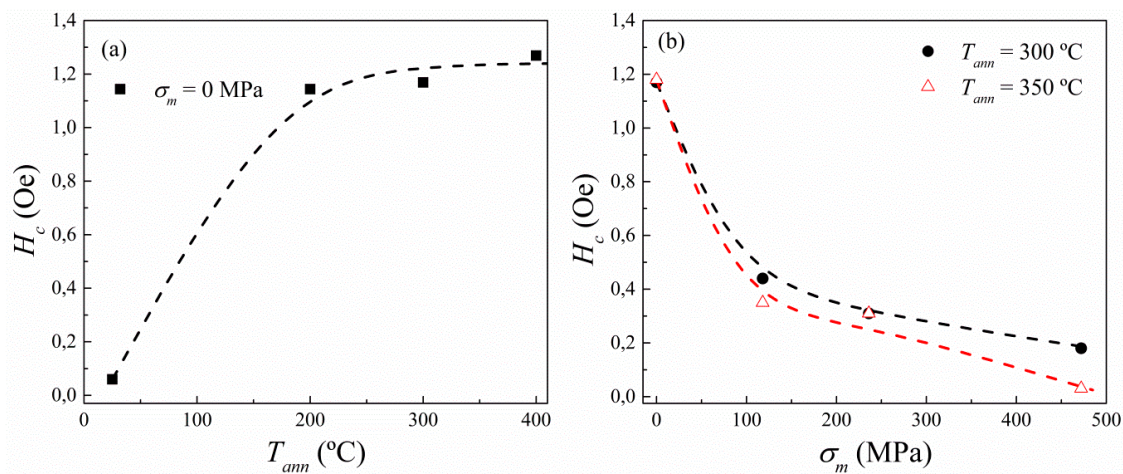


Figure 2. Temperature-annealing (a) and stress-annealing (b) dependence on the H_c of $\text{Co}_{69.2}\text{Fe}_{3.6}\text{Ni}_1\text{B}_{12.5}\text{Si}_{11}\text{Mo}_{1.5}\text{C}_{1.2}$ microwires for 1 h of thermal-treatment. Dashed lines are a guide to the eyes.

In Figure 3 we confirm the dissimilar effect of conventional annealing on the GMI response depending on T_{ann} . On the one hand, Figure 3a shows a reduction in the GMI ratio upon annealing at 200 °C, decreasing from 103% (for the as-prepared) down to 62% at 100 MHz. However, a clear improvement in the GMI effect is achieved when annealing at 300 °C, rising from 103% up to 141% at 100 MHz. Furthermore, despite the opposite effect of conventional annealing on the GMI response, it is noteworthy that in Figure 3c the maximum value of the $\Delta Z/Z_{max}$ ratio is monotonously shifted to high-frequencies as the T_{ann} rises. This characteristic frequency, hereinafter f_{char} , is defined as the frequency at which the $\Delta Z/Z_{max}$ ratio is maximal. In addition, in Figure 3d the field sensitivity displays minor differences in the frequency dependence between samples. Therefore, conventional annealing is revealed as an adequate treatment to improve the GMI response only at certain annealing conditions.

With regard to the effect of stress-annealing on the GMI response, in Figure 4 it is clearly appreciated as a significant GMI improvement as compared to conventional annealing for all stress-annealed microwires. For example, the measured $\Delta Z/Z$ ratio of the as-prepared microwire is equal to 103% at 100 MHz, whereas an increase up to 166% is found in the stress-annealed microwire at 200 °C and 118 MPa (see Figure 4a). By contrast, a reduction in the $\Delta Z/Z$ ratio down to 62% is observed in Figure 3a for the conventional annealed microwire at 200 °C. The improvement in the GMI response clearly is stated in Figure 4c for the whole frequency range (up to 1000 MHz). Moreover, Figure 4c shows a slight increase in f_{char} up to ca. 150 MHz for the $\Delta Z/Z_{max}$ of the stress-annealed microwires, in comparison with the as-prepared microwire where the maximum is centred at ca. 80 MHz. Figure 4d draws a clear improvement in the field sensitivity for the stress-annealed samples, in contrast to conventional annealing. Particularly, at 100 MHz, the field sensitivity rises from 10%/Oe for the as-prepared, up to $\eta = 64\%$ /Oe when stress-annealing at 300 °C and 118 MPa. However, the field sensitivity obtained for the three stress-annealed samples is quite similar in the frequency range $500 \leq f \leq 1000$ MHz. In fact, they follow the same tendency as those shown in Figure 4c for the frequency dependence of $\Delta Z/Z_{max}$. In summary, stress-annealing arises here as the suitable technique to enhance simultaneously the GMI ratio and field sensitivity.

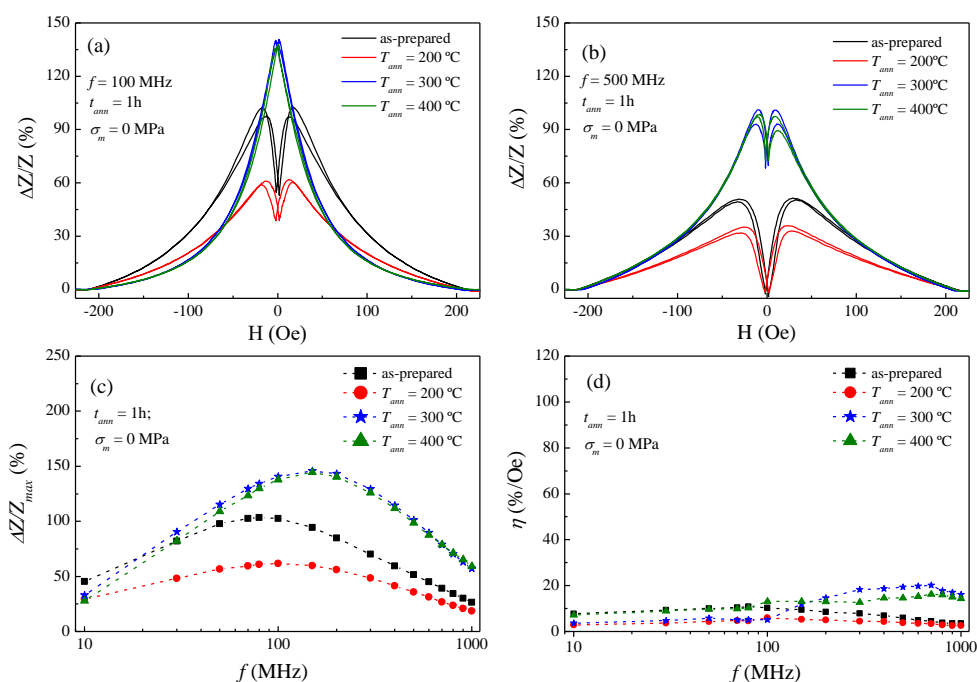


Figure 3. Field dependence of the GMI ratio for the as-prepared and annealed $\text{Co}_{69.2}\text{Fe}_{3.6}\text{Ni}_1\text{B}_{12.5}\text{Si}_{11}\text{Mo}_{1.5}\text{C}_{1.2}$ microwires measured at representative frequencies: (a) 100 MHz and (b) 500 MHz; (c) frequency dependence of $\Delta Z/Z_{\max}$, and (d) field sensitivity. Dashed-lines in (c) and (d) are a guide to the eye, while full-symbols denote experimental data.

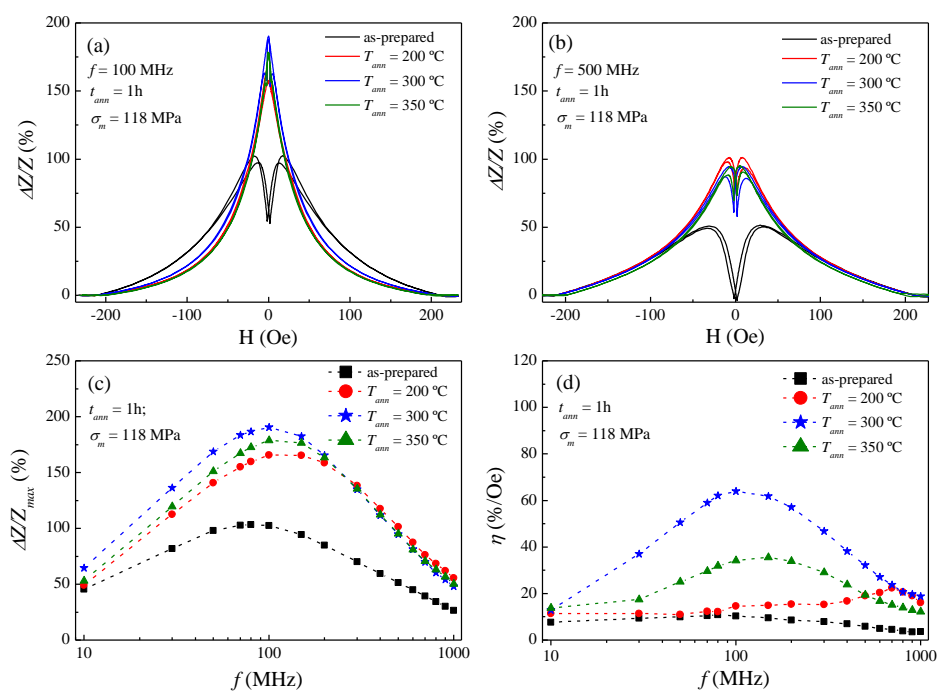


Figure 4. Field dependence of the GMI ratio for the as-prepared and 118 MPa stress-annealed $\text{Co}_{69.2}\text{Fe}_{3.6}\text{Ni}_1\text{B}_{12.5}\text{Si}_{11}\text{Mo}_{1.5}\text{C}_{1.2}$ microwires measured at representative frequencies: (a) 100 MHz and (b) 500 MHz; (c) frequency dependence of $\Delta Z/Z_{\max}$, and (d) field sensitivity. Dashed-lines in (c,d) are a guide to the eye, while full-symbols denote experimental data.

In this line, the 118 MPa stress-annealed microwire at 300 °C presents the highest GMI response and field sensitivity, as show in Figure 4c,d, respectively. For this reason, it was resolved to make

a more detailed investigation of the stress-annealing effect under different applied stresses, but at a fixed T_{ann} of 300 °C (see Figure 5). It is worth noticing the remarkable improvement of both the GMI effect and field sensitivity, though at different stress-annealing treatments. Figure 5c shows the positive evolution of $\Delta Z/Z_{max}$ as the applied stress σ_m rises. In fact, this positive change is even more evident in the field sensitivity response (see Figure 5d). Specifically, at 100 MHz the GMI ratio improves up to 234% for an applied stress of 236 MPa, in contrast to the 103% for the as-prepared sample. On the other hand, the field sensitivity is enhanced up to 104%/Oe for the 472 MPa stress-annealed microwire, while the as-prepared exhibits a poor 10%/Oe. Therefore, the field sensitivity improves as the applied stress rises (see Figure 5d) within the following range $10 \text{ MHz} \leq f \leq 200 \text{ MHz}$. This frequency range is the preferred for sensors applications because of better signal to noise features and hence lower price of electronic circuits, allowing easier processing of the electronic signals [17]. In short, this makes our stress-annealed sample a suitable material for sensor applications [9]. It is worth noting that for other families of thicker Co-rich wires ($d = 120 \mu\text{m}$) prepared by the in-rotating water technique a $f_{char} < 1 \text{ MHz}$ has been reported [42].

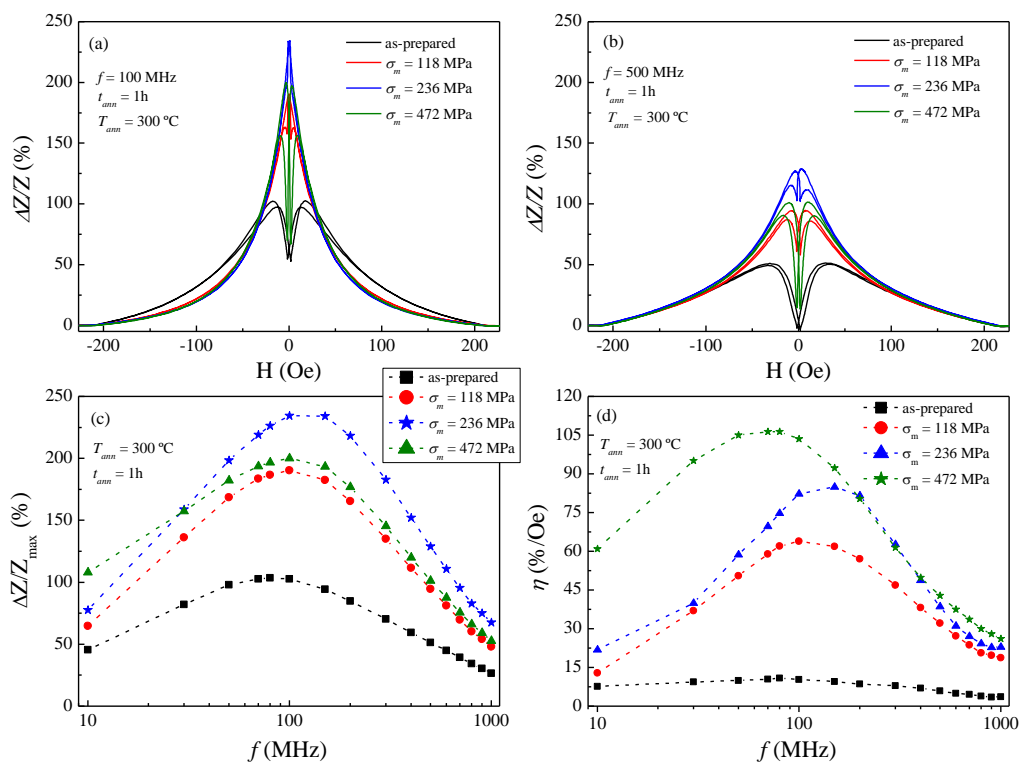


Figure 5. Field dependence of the GMI ratio for the as-prepared and stress-annealed $\text{Co}_{69.2}\text{Fe}_{3.6}\text{Ni}_1\text{B}_{12.5}\text{Si}_{11}\text{Mo}_{1.5}\text{C}_{1.2}$ microwires measured at $300 \text{ }^\circ\text{C}$: (a) 100 MHz and (b) 500 MHz; (c) frequency dependence of $\Delta Z/Z_{max}$, and (d) field sensitivity. Dashed-lines in (c,d) are a guide to the eye, while full-symbols denote experimental data.

All the experimental results reported here could be described considering that the origin of the GMI effect is directly connected to the skin depth (ac frequency f) and the circumferential magnetic permeability (through the external dc magnetic field H_{dc} , ac current, and induced anisotropies). Consequently, a good understanding of both features is a requirement for high-performance soft magnetic materials [13]. In fact, it is well-known that both skin depth and circumferential permeability are interrelated, and in magnetic microwires of radius a can be given as follows [24,42,43]:

$$\delta_m = \frac{1}{\sqrt{\pi \sigma \mu_\phi f}} \quad (4)$$

where σ and μ_ϕ are the electrical conductivity and circumferential magnetic permeability, respectively.

In view of this, we can tackle the GMI response by drawing a general description of skin effect and magnetic anisotropy. The frequency studied in this paper covers the frequency range from 10 to 1000 MHz, in which the skin depth δ_m plays an important role. In panels (a) and (b) of Figures 3–5, the GMI exhibits the expected double-peak behaviour for the as-prepared sample (in the whole frequency range), which results from the induced magnetoelastic anisotropy during the fabrication. By contrast, at 100 MHz a single-peak response is achieved by specific conventional annealing (at $T_{ann} \geq 300$ °C in Figure 3a) and stress-annealed samples ($\sigma_m \leq 236$ MPa in Figures 4a and 5a, respectively). This is the result of vanishing induced magnetoelastic anisotropies during their fabrication. Moreover, in annealed and stress-annealed samples (at low σ_m -values) the internal stresses' relaxation contributes to the axial anisotropy, and therefore, GMI response tends to be single-peak. However, in stress-annealed samples, at sufficiently high σ_m -values, the circumferential anisotropy becomes more relevant and double-peak behaviour is observed at 100 MHz. In addition, at 500 MHz all the treated samples exhibit double-peak behaviour. Once more, this is straightforward explained through the frequency dependence of the skin effect in magnetic microwires (see Equation (4)), while the influence of magnetoelastic anisotropies are taken into consideration. In this sense, at relatively low frequencies, it is assumed that the current flows through the whole ferromagnetic nucleus, i.e., the skin depth is comparable to the microwire radius, i.e., $\delta_m \approx a$ [33,44]. However, as frequencies increase, the skin depth decreases and hence the current flows closer to the surface while inducing the circumferential magnetic anisotropy near the metallic nucleus surface, which in turn becomes more relevant. For that reason, it is expected a magnetic evolution from single to double-peak behaviour in the GMI response for some of the samples considered in this study.

Regarding the key role of the skin effect in the GMI response, where $Z \sim 1/\delta_m$ [43,44], in Figure 6 we show the penetration skin depth dependence of $(\Delta Z/Z)_{max}$. The skin depth δ_m has been estimated through Equation (5) by considering that the real component of the measured impedance stems from the variations of the effective surface where the ac-current flows as a result of the skin effect [44–46]. This approach connects δ_m with the ratio R_{DC}/R_{AC} , as follows:

$$\delta_m = a \left[1 - \left(1 - \frac{R_{DC}}{R_{AC}} \right)^{1/2} \right] \quad (5)$$

where R_{DC} is the dc-resistance of the wire, and R_{AC} is the real component of the measured impedance at a given frequency as a function of the axially applied dc-field, and a is the wire radius. The minimum skin depth δ_m^{min} represented in Figure 6 is obtained from Equation (5) for each frequency in all samples.

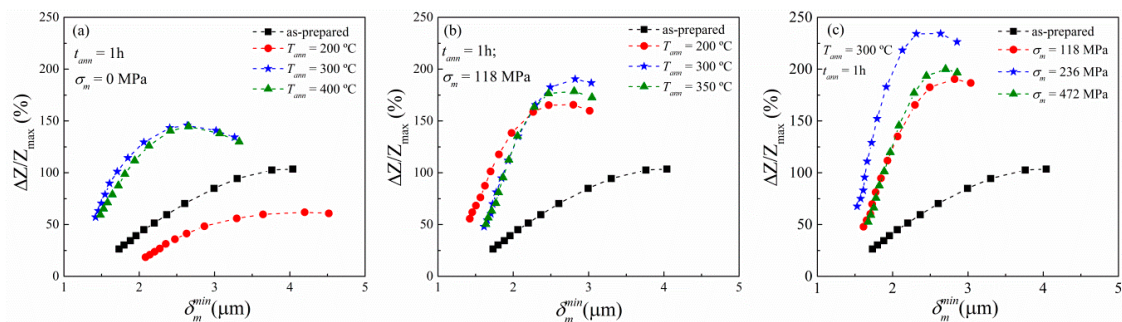


Figure 6. Minimum skin depth dependence of $(\Delta Z/Z)_{max}$ for as-prepared and conventional annealed (a), as-prepared and stress-annealed at a fixed σ_m of 118 MPa while varying the T_{ann} (b), and at a fixed annealing temperature while varying the applied stress (c) for the $\text{Co}_{69.2}\text{Fe}_{3.6}\text{Ni}_1\text{B}_{12.5}\text{Si}_{11}\text{Mo}_{1.5}\text{C}_{1.2}$ microwires. Dashed-lines are a guide to the eye, while full-symbols denote experimental data. The frequency dependence increases from right to left in contrast to panel (c) of Figures 3–5.

Although, the $(\Delta Z/Z)_{\max}$ represented here redraws the same tendency as in the panel (c) of Figures 3–5, that is, the increment (or diminishing for the conventional annealed sample at 200 °C) in the GMI effect depending on the treatment. In Figure 6 the treatment effect on the GMI response is more clearly evident. As a general rule of thumb, the treatment efficiency is directly related to the reduction of the δ_m^{\min} while the GMI effect is improved. Thus, the skin depth not only gives a direct hint of the (positive/negative) influence of the treatment in the GMI response but also delimits the range of efficacy.

As mentioned above, the GMI response relies on the skin effect. Moreover, this effect only becomes relevant when $\delta_m \lesssim a$, that is, in the intermediate frequency range where the maximal $(\Delta Z/Z)_{\max}$ is expected to occur [13,25]. Bear in mind that f_{char} is defined as the frequency at which the GMI response is maximal. Taking this into consideration along with Equation (4), we obtain the following qualitative expression for the f_{char} [43,44]:

$$f_{char} = \frac{1}{\pi \mu_{\phi} \sigma a^2} \quad (6)$$

From Equation (6) it is inferred that the higher the circumferential magnetic permeability, the lower the f_{char} . This is experimentally evinced in panel (c) of Figures 3–5. Specifically, in Figure 3c the as-prepared sample exhibits the f_{char} at 80 MHz, whereas the conventional annealed samples show the maximal GMI response at a higher f_{char} , i.e., 100 MHz for the T_{ann} at 200 °C and 150 MHz for the T_{ann} samples at 300 and 400 °C. Similarly, Figures 4c and 5c display the same tendency for the f_{char} . In this sense, all the treated samples presented in this work show an increase in the f_{char} as a result of the gradual internal-stresses relaxation that contributes to the axial anisotropy, but at the expense of the circumferential anisotropy.

Field sensitivity is represented in panel (d) of Figures 3–5. There it is noticed the positive effect the stress-annealing on field sensitivity in Figure 5d. This could be derived either from the induced magnetoelastic anisotropy upon stress-annealing, or even from a change in the magnetostriction coefficient. Furthermore, Figure 4d shows an improvement in the sensitivity as the T_{ann} rises up to a critical value of 300 °C. Above this temperature, the sensitivity is reduced. We surmise this counterbalance effect as a consequence of inner stress relaxation, i.e., the annealing above 300 °C vanishes the magnetoelastic anisotropy in the microwire, which in turn is negatively reflected in both GMI response and field sensitivity.

Finally, microwires with different chemical composition and internal stresses (to a great extent related to the thickness of the glass-coating [30,31]) must present distinct GMI performance. However, similar effects of conventional annealing on the magnetic properties of Co-rich microwires of different chemical composition have already been reported, i.e., a significant magnetic hardening in various Co-based microwires with vanishing λ_s -values has been noticed upon applying a conventional annealing [32]. Such magnetic hardening negatively affects the GMI performance [26,27,32]. In the present case, we have identified the precise route that enhances the GMI response and field sensitivity in the studied microwire with a well-established chemical composition. We anticipate that experimental dependencies concerning Co-rich microwires will be disclosed in the near future.

4. Conclusions

In summary, we have performed a comprehensive investigation of the GMI response and the field sensitivity by modifying the magnetoelastic anisotropies through different thermal treatments (conventional and stress-annealing) on the ferromagnetic amorphous $\text{Co}_{69.2}\text{Fe}_{3.6}\text{Ni}_1\text{B}_{12.5}\text{Si}_{11}\text{Mo}_{1.5}\text{C}_{1.2}$ glass-coated microwire. On the one hand, the findings reported reveal stress-annealing as the suitable technique to improve simultaneously and remarkably the GMI effect and the field sensitivity. In this sense, it is observed a maximum GMI response of 234% for the exciting current frequency of 100 MHz and a maximum field sensitivity of 104%/Oe for the 300 °C stress-annealing sample at 236 and 472 MPa, respectively. Moreover, a significant frequency dependence of field sensitivity is attained in the stress-annealed samples. These results have been discussed in terms of the frequency dependence of

skin depth, along with the magnetoelastic anisotropy modification. The presented outcomes can be used as a guide in further studies while deepening the knowledge to draw future lines in materials design. Hence, we evinced the stress-annealed $\text{Co}_{69.2}\text{Fe}_{3.6}\text{Ni}_1\text{B}_{12.5}\text{Si}_{11}\text{Mo}_{1.5}\text{C}_{1.2}$ glass-coated microwire as a prospective material for sensor applications.

Author Contributions: D.G.-A. and L.G.-L. wrote the manuscript; V.Z., L.G.-L. and P.C.-L. prepared and annealed the samples; M.I., V.Z., J.M.B., L.G.-L. and P.C.-L. performed the magnetic and GMI measurements; L.G.-L., D.G.-A. and A.Z. participated in the result analysis and discussion. All the authors reviewed and finalized the manuscript. All authors have read and agreed to the published version of the manuscript.

Funding: D.G.-A is founded by MAT2017-83631-C3-R. This work was also supported by Spanish MCIU under PGC2018-099530-B-C31 (MCIU/AEI/FEDER, UE) and by the Government of the Basque Country under PIBA 2018-44 project and by the University of Basque Country under the scheme of “Ayuda a Grupos Consolidados” (Ref.: GIU18/192).

Acknowledgments: Authors give thanks for technical and human support to SGiker of UPV/EHU (Medidas Magnéticas Gipuzcoa) and European funding (ERDF and ESF).

Conflicts of Interest: Authors declare no conflict of interest.

References

- Díaz-Michelena, M. Small Magnetic Sensors for Space Applications. *Sensors* **2009**, *9*, 2271–2283. [[CrossRef](#)]
- Nowicki, M.; Szweczyk, R. Determination of the Location and Magnetic Moment of Ferromagnetic Objects Based on the Analysis of Magnetovision Measurements. *Sensors* **2019**, *19*, 337. [[CrossRef](#)]
- Lenz, J.; Edelstein, A.S. Magnetic Sensors and their applications. *IEEE Sens. J.* **2006**, *6*, 631–649. [[CrossRef](#)]
- Mohri, K.; Uchiyama, T.; Panina, L.V. Recent advances of micro magnetic sensors and sensing application. *Sens. Actuators A* **1997**, *59*, 1–8. [[CrossRef](#)]
- Kozejova, D.; Fecova, L.; Klein, P.; Sabol, R.; Hudak, R.; Sulla, I.; Mudronova, D.; Galik, J.; Varga, R. Biomedical applications of glass-coated microwires. *J. Magn. Magn. Mater.* **2019**, *470*, 2–5. [[CrossRef](#)]
- Morales, I.; Archilla, D.; de la Presa, P.; Hernando, A.; Marin, P. Colossal heating efficiency via Eddy currents in amorphous microwires with nearly zero magnetostriction. *Sci. Rep.* **2020**, *10*, 602. [[CrossRef](#)] [[PubMed](#)]
- Panina, L.V.; Mohri, K. Magneto-impedance effect in amorphous wires. *Appl. Phys. Lett.* **1994**, *65*, 1189–1191. [[CrossRef](#)]
- Panina, L.V.; Mohri, K.; Uchiyama, T.; Noda, M. Giant Magneto-Impedance in Co-Rich Amorphous Wires and Films. *IEEE Trans. Magn.* **1995**, *31*, 1249. [[CrossRef](#)]
- Hauser, M.; Kraus, L.; Ripka, P. Giant magnetoimpedance sensors. *IEEE Instrum. Meas. Mag.* **2001**, *4*, 28–32. [[CrossRef](#)]
- Ripka, P.; Vertesy, G. Sensors based on soft magnetic materials Panel discussion. *J. Magn. Magn. Mater.* **2000**, *215*, 795–799. [[CrossRef](#)]
- Jiles, D.C. Recent advances and future directions in magnetic materials. *Acta Mater.* **2003**, *51*, 5907–5939. [[CrossRef](#)]
- Panina, L.V.; Makhnovskiy, D.P.; Dzhumazoda, A.; Podgornaya, S.V. High Performance Soft Magnetic Materials. In *Springer Series in Materials Science*; Zhukov, A., Ed.; Springer International Publishing: Cham, Switzerland, 2017; p. 216. ISBN 0933-033X.
- Kraus, L.; Vázquez, M.; Knobel, M. Giant Magnetoimpedance. In *Handbook of Magnetic Materials*; Elsevier: Amsterdam, The Netherlands, 2003; p. 497, ISSN: 1567-2719.
- Pirota, K.R.; Kraus, L.; Chiriach, H.; Knobel, M. Magnetic properties and giant magnetoimpedance in CoFeSiB glass-covered microwires. *J. Magn. Magn. Mater.* **2000**, *221*, L243–L247. [[CrossRef](#)]
- Zhukov, A.; Zhukova, V.; Blanco, J.M.; Gonzalez, J. Recent research on magnetic properties of glass-coated microwires. *J. Magn. Magn. Mater.* **2005**, *294*, 182–192. [[CrossRef](#)]
- Mohri, K.; Uchiyama, T.; Panina, L.V.; Yamamoto, M.; Bushida, K. Recent Advances of Amorphous Wire CMOS IC Magneto-Impedance Sensors: Innovative High-Performance Micromagnetic Sensor Chip. *J. Sens.* **2015**, *2015*, 718069. [[CrossRef](#)]
- Dufay, B.; Saez, S.; Dolabdjian, C.; Melo, L.G.C.; Yelon, A.; Ménard, D. Development of a high sensitivity Giant Magneto-Impedance magnetometer: Comparison with a commercial Flux-Gate. *IEEE Trans. Magn.* **2013**, *49*, 85. [[CrossRef](#)]

18. Uchiyama, T.; Mohri, K.; Nakayama, S. Measurement of Spontaneous Oscillatory Magnetic Field of Guinea-Pig Smooth Muscle Preparation Using Pico-Tesla Resolution Amorphous Wire Magneto-Impedance Sensor. *IEEE Trans. Magn.* **2011**, *47*, 3070–3073. [[CrossRef](#)]
19. Chen, L.; Bao, C.C.; Yang, H.; Li, D.; Lei, C.; Wang, T.; Hu, H.Y.; He, M.; Zhou, Y.; Cui, D.X. A prototype of giant magnetoimpedance-based biosensing system for targeted detection of gastric cancer cells. *Biosens. Bioelectron.* **2011**, *26*, 3246–3253. [[CrossRef](#)]
20. Ulitovskiy, A.V.; Maianski, I.M.; Avramenco, A.I. Method of Continuous Casting of Glass Coated Microwire. USSR Patent No. 128427, 15 May 1960. p. 14.
21. Zhukov, A.; Ipatov, M.; Corte-León, P.; Gonzalez-Legarreta, L.; Churyukanova, M.; Blanco, J.M.; Gonzalez, J.; Taskaev, S.; Hernando, B.; Zhukova, V. Giant magnetoimpedance in rapidly quenched materials. *J. Alloy Compd.* **2020**, *814*, 152225. [[CrossRef](#)]
22. Sandacci, S.; Makhnovskiy, D.; Panina, L.; Larin, V. Stress-dependent magnetoimpedance in Co-based amorphous wires with induced axial anisotropy for tunable microwave composites. *IEEE Trans. Magn.* **2005**, *41*, 3553–3555. [[CrossRef](#)]
23. Zhukov, A.; Talaat, A.; Churyukanova, M.; Kaloshkin, S.; Semenkova, V.; Ipatov, I.; Blanco, J.M.; Zhukova, V. Engineering of magnetic properties and GMI effect in Co-rich amorphous microwires. *J. Alloy. Comp.* **2016**, *664*, 235–241. [[CrossRef](#)]
24. Panina, L.V.; Mohri, K.; Bushida, K.; Noda, M. Giant magnetoimpedance and magnetoinductive effects in amorphous alloys. *J. Appl. Phys.* **1994**, *76*, 6198. [[CrossRef](#)]
25. Phan, M.H.; Peng, H.X. Giant magnetoimpedance materials: Fundamentals and applications. *Prog. Mater. Sci.* **2008**, *53*, 323–420. [[CrossRef](#)]
26. Zhukov, A.; Ipatov, M.; Zhukova, V. Advances in Giant Magnetoimpedance of Materials. In *Handbook of Magnetic Materials*; Buschow, K.H.J., Ed.; Elsevier: Amsterdam, The Netherlands, 2015; Volume 24, pp. 139–236.
27. Zhukov, A.; Ipatov, M.; Corte-León, P.; González-Legarreta, L.; Blanco, J.M.; Zhukova, V. Soft magnetic microwires for sensor applications. *J. Magn. Magn. Mater.* **2020**, *498*, 166180. [[CrossRef](#)]
28. Zhukov, A.; Churyukanova, M.; Kaloshkin, S.; Sudarchikova, V.; Gudoshnikov, S.; Ipatov, M.; Talaat, A.; Blanco, J.M.; Zhukova, V. Magnetostriction of Co-Fe-based amorphous soft magnetic microwires. *J. Electr. Mater.* **2016**, *45*, 226–234. [[CrossRef](#)]
29. Konno, Y.; Mohri, K. Magnetostriction measurements for amorphous wires. *IEEE Trans. Magn.* **1989**, *25*, 3623–3625. [[CrossRef](#)]
30. Zhukov, A.; Gonzalez, J.; Torcunov, A.; Pina, E.; Prieto, M.J.; Cobeño, A.F.; Blanco, J.M.; Larin, S.; Baranov, V. Ferromagnetic resonance and Structure of Fe-based Glass-coated Microwires. *J. Magn. Magn. Mater.* **1999**, *203*, 238–240. [[CrossRef](#)]
31. Chiriac, H.; Óvári, T.-A.; Corodeanu, S.; Ababei, G. Interdomain wall in amorphous glass-coated microwires. *Phys. Rev. B* **2007**, *76*, 214433. [[CrossRef](#)]
32. Zhukova, V.; Ipatov, M.; Talaat, A.; Blanco, J.M.; Churyukanova, M.; Zhukov, A. Effect of stress annealing on magnetic properties and GMI effect of Co- and Fe-rich microwires. *J. Alloys Compd.* **2017**, *707*, 189–194. [[CrossRef](#)]
33. Gonzalez-Legarreta, L.; Corte-Leon, P.; Zhukova, V.; Ipatov, M.; Blanco, J.M.; Gonzalez, J.; Zhukov, A. Optimization of magnetic properties and GMI effect of Thin Co-rich Microwires for GMI Microsensors. *Sensors* **2020**, *20*, 1588. [[CrossRef](#)]
34. Zhukova, V.; Corte-Leon, P.; Ipatov, M.; Blanco, J.M.; González-Legarreta, L.; Zhukov, A. Development of Magnetic Microwires for Magnetic Sensor Applications. *Sensors* **2019**, *19*, 4767. [[CrossRef](#)] [[PubMed](#)]
35. Gonzalez-Legarreta, L.; Corte-León, P.; Zhukova, V.; Ipatov, M.; Blanco, J.M.; Churyukanova, M.; Taskaev, S.; Zhukov, A. Route of magnetoimpedance and domain walls dynamics optimization in Co-based microwires. *J. Alloy. Compd.* **2020**, *830*, 154576. [[CrossRef](#)]
36. Zhukova, V.; Cobeño, A.F.; Zhukov, A.; de Arellano Lopez, A.R.; López-Pombero, S.; Blanco, J.M.; Larin, V.; Gonzalez, J. Correlation between magnetic and mechanical properties of devitrified glass-coated Fe_{71.8}Cu₁Nb_{3.1}Si₁₅B_{9.1} microwires. *J. Magn. Magn. Mater.* **2002**, *249*, 79–84. [[CrossRef](#)]
37. Zhukova, V.; Cobeño, A.F.; Zhukov, A.; Blanco, J.M.; Puerta, S.; Gonzalez, J.; Vázquez, M. Tailoring of magnetic properties of glass coated microwires by current annealing. *J. Non-Cryst. Solids* **2001**, *287*, 31–36. [[CrossRef](#)]

38. Zhukova, V.; Blanco, J.M.; Ipatov, M.; Churyukanova, M.; Taskaev, S.; Zhukov, A. Tailoring of magnetoimpedance effect and magnetic softness of Fe-rich glass-coated microwires by stress- annealing. *Sci. Rep.* **2018**, *8*, 3202. [[CrossRef](#)]
39. Zhukov, A.; Chichay, K.; Talaat, A.; Rodionova, V.; Blanco, J.M.; Ipatov, M.; Zhukova, V. Manipulation of magnetic properties of glass-coated microwires by annealing. *J. Magn. Magn. Mater.* **2015**, *383*, 232–236. [[CrossRef](#)]
40. Churyukanova, M.; Semenkova, V.; Kaloshkin, S.; Shuvaeva, E.; Gudoshnikov, S.; Zhukova, V.; Shchetinin, I.; Zhukov, A. Magnetostriction investigation of soft magnetic microwires. *Phys. Status Solidi A* **2016**, *213*, 363–367. [[CrossRef](#)]
41. Cobeño, A.F.; Zhukov, A.; Blanco, J.M.; Larin, V.; Gonzalez, J. Magnetoelastic sensor based on GMI of amorphous microwire. *Sens. Actuators A* **2001**, *91*, 95–98. [[CrossRef](#)]
42. Aragonese, P.; Zhukov, A.; Gonzalez, J.; Blanco, J.M.; Dominguez, L. Effect of AC driving current on Magneto-Impedance effect. *Sens. Actuators A* **2000**, *81*, 86–90. [[CrossRef](#)]
43. Mishra, A.C.; Sahoo, T.; Srinivas, V.; Thakur, A.K. Giant magnetoimpedance in electrodeposited CoNiFe/Cu wire: A study on thickness dependence. *J. Alloys Compd.* **2009**, *480*, 771. [[CrossRef](#)]
44. Lachowicz, H.K.; Garcia, K.L.; Kuzminski, M.; Zhukov, A.; Vazquez, M. Skin-effect and circumferential permeability in micro-wires utilized in GMI-sensors. *Sens. Actuators A* **2005**, *119*, 384–389. [[CrossRef](#)]
45. Zhukov, A.; Talaat, A.; Ipatov, M.; Granovsky, A.; Zhukova, V. Estimation of the frequency and magnetic field dependence of the skin depth in Co-rich magnetic microwires from GMI experiments. *J. Sci. Adv. Mater. Devices* **2016**, *1*, 388–392. [[CrossRef](#)]
46. Knobel, M.; Sanches, M.L.; Gomez-Polo, C.; Marin, P.; Vazquez, M.; Hernando, A. Giant magneto-impedance effect in nanostructured magnetic wires. *J. Appl. Phys.* **1996**, *79*, 1646–1654. [[CrossRef](#)]



© 2020 by the authors. Licensee MDPI, Basel, Switzerland. This article is an open access article distributed under the terms and conditions of the Creative Commons Attribution (CC BY) license (<http://creativecommons.org/licenses/by/4.0/>).